RevMexAA (Serie de Conferencias), **15**, 166–171 (2003)

CHAMPAGNE FLOWS AND WINDS IN H II REGIONS

S. Lizano,[1] D. Galli,[2] F. Shu,[3] and J. Cantó[4]

RESUMEN

Discutimos la expansión de un núcleo molecular autogravitante singular inicialmente en equilibrio caracterizado por una distribución de densidad como ley de potencia del radio, $\rho \propto r^{-n}$ con $3/2 < n < 3$. Este núcleo es calentado fuera de equilibrio mecánico por la formación de una estrella masiva en su centro. Si la ionización y calentamiento iniciales ocurren a $t = 0$, el flujo subsecuente para $r \gg 100$ AU, causado por la falta de balance entre la autogravedad y la presión térmica, es autosimilar. Debido al empinado perfil de densidad, los gradientes de presión producen un choque que viaja a través de la nube, acelerando el gas a velocidades supersónicas en lo que ha sido llamada la "fase de champán". La expansión de la región interna a $t > 0$ esta conectada a la envolvente externa de la nube ionizada a través de este choque, cuya intensidad es una función creciente del exponente n. Además, discutimos la evolución de los fuertes vientos de las estrellas masivas dentro de estos flujos de champán.

ABSTRACT

We discuss the expansion of an initially self-gravitating, static, singular cloud core characterized by a power-law density distribution, $\rho \propto r^{-n}$, with $3/2 < n < 3$. This core is heated out of mechanical balance by the formation of a massive star at its center. If the initial ionization and heating is approximated to occur instantaneously at $t = 0$, the subsequent flow (for $r \gg 100\,$AU) caused by the resulting imbalance between self-gravity and thermal pressure is self-similar. Because of the steep density profile, pressure gradients produce a shock front that travels into the cloud, accelerating the gas to supersonic velocities in what has been called the "champagne phase". The expansion of the inner region at $t > 0$ is connected to the outer envelope of the now ionized cloud core through this shock whose strength is an increasing function of the exponent n. We also discuss the evolution of the strong stellar winds of massive stars inside these champagne flows.

Key Words: **HII REGIONS — STARS: FORMATION — STARS: MASS LOSS**

1. INTRODUCTION

Recently, Shu et al. (2002; hereafter SLGCL) found self-similar solutions for the expansion of molecular cloud cores with power-law density distributions that are heated out of mechanical balance by the formation of a massive star at the center. In this paper we will discuss part of their results and also the evolution of the powerful stellar winds in the champagne flows.

For a spherically symmetric molecular cloud core, initially at rest, the size r_S of the region that can be ionized is given by the standard formula (Strömgren 1939):

$$\int_{r_0}^{r_S} n_e n_p\, \alpha_2\, 4\pi r^2\, dr = \dot{N}_*. \tag{1}$$

Equation (1) assumes ionization equilibrium and the "on-the-spot" approximation. In the above, n_e is the electron density, n_p is the ion density, α_2 is the recombination coefficient to the second energy level of hydrogen, $\dot{N}_*$ is the rate of ionizing photons from the star (assumed to be a constant) and r_0 is the radius below which all of the gas in the original cloud core may be considered to have fallen into the center (perhaps via a disk) to make a star of mass M_*. If the virial velocity (thermal, turbulent, or magnetohydrodynamic) supporting the original (neutral) cloud core before star formation is denoted by a_1, order of magnitude arguments yield $r_0 \sim r_1$, the Bondi-Parker radius of this neutral gas,

$$r_1 \equiv \frac{GM_*}{2a_1^2}. \tag{2}$$

The square of the sound speed in the H II gas a_2^2 is generally appreciably larger than a_1^2, thus, the equivalent Bondi-Parker radius of the ionized gas,

$$r_2 \equiv \frac{GM_*}{2a_2^2}, \tag{3}$$

will be considerably smaller than r_1.

[1]Instituto de Astronomía, UNAM, Morelia, México.
[2]Osservatorio di Arcetri, Florence, Italy.
[3]National Tsing Hua University, Hsinchu, Taiwan.
[1]Instituto de Astronomía, UNAM, México D.F., México.

For typical numbers, $M_* \simeq 25\,M_\odot$, $a_1 \simeq 1\,\mathrm{km\,s^{-1}}$, $a_2 \simeq 10\,\mathrm{km\,s^{-1}}$, we have $r_1 \simeq 10^4$ AU $\gg r_2 \simeq 10^2$ AU, with both r_1 and r_2 much bigger than the physical radius of the star. Much interior to r_2, the ionized gas will empty into the star (or more likely, into a disk if it has even a slight amount of angular momentum), whereas much exterior to r_2, the gravitationally unbound H II gas will expand outward, if it has not already reached pressure equilibrium with the surrounding cloud. Since $r_0 \gg r_2$, one can ignore the gravitational field of the star on the flow of the H II region beyond r_0.

Assume now that the molecular cloud core initially had a power-law distribution of gas density

$$\rho(r) = K r^{-n}. \tag{4}$$

If $n < 3/2$, the ultraviolet radiation is trapped within a finite radius r_S, and the H II region is said to be "ionization bounded" (see Osterbrock 1989). If $n > 3/2$, the H II region can be either ionization bounded or "density bounded". In the latter case, a finite output of ultraviolet radiation can ionize an infinite volume of gas beyond r_0. The dividing line between being ionization bounded and density bounded arises when the density constant K equals a critical value K_cr:

$$K_\mathrm{cr} = 2\mu_\mathrm{i}\, m_\mathrm{H} \left[\frac{(2n-3)\, r_0^{2n-3}\, \dot{N}_*}{4\pi\, \alpha_2}\right]^{1/2}, \tag{5}$$

where μ_i is the mean weight per particle of the ionized gas, m_H is the hydrogen mass, and $n_\mathrm{p} = n_\mathrm{e} = \rho/2\mu_\mathrm{i} m_\mathrm{H}$.

One can compare the value of K_cr with the value K_* implied by the assumption that the power law (equation 4) initially extended inward from r_0 as well as outward, but that the part inward of r_0 has fallen into the center to make a star of mass M_*:

$$K_* = \frac{(3-n)\, M_*}{4\pi\, r_0^{3-n}}. \tag{6}$$

Taking the ratio of equations (6) and (5), we get

$$\frac{K_*}{K_\mathrm{cr}} = \left[\frac{(3-n)\, M_*}{2\mu_\mathrm{i}\, m_\mathrm{H}}\right] \left[\frac{\alpha_2}{(2n-3)\, 4\pi r_0^3\, \dot{N}_*}\right]^{1/2}. \tag{7}$$

For $M_* \simeq 25\,M_\odot$, $r_0 \simeq 10^4$ AU, $\dot{N}_* \simeq 10^{49}\,\mathrm{s^{-1}}$, $\alpha_2 \simeq 2.6\times10^{-13}\,\mathrm{cm^3\,s^{-1}}$, $K_*/K_\mathrm{cr} \simeq 23\,(3-n)/(2n-3)^{1/2}$.

Since K_* represents a rough estimate of K and $K_* > K_\mathrm{cr}$, this calculation indicates that the H II regions of $25\,M_\odot$ (and lower mass) stars are likely to be ionization bounded, at least initially before any expansion occurs. However, if we assume that $\dot{N}_*$ scales roughly as M_*^3 (as indicated by the results of Vacca et al. 1996), the expression on the right-hand side scales as M_*^{-2}, indicating that the H II regions of the most massive O stars may be density bounded from the start, especially if such stars are born in regions with density gradients close to $n = 3$. They will then develop champagne flows as follows.

When $K \sim K_* < K_\mathrm{cr}$, the ionization front (IF) created by the idealized instantaneous appearance of a star at $t = 0$ rapidly moves to infinity and establishes an isothermal structure with $T \simeq 10^4$ K. After the passage of the IF, the cloud remains out of mechanical balance and the pressure gradients will produce an expansion of the whole cloud. Due to the density gradient the inner regions expand faster than the outer regions and a shock travels through the cloud, accelerating the gas to supersonic velocities. This is known as the "champagne phase" (e.g., Bodenheimer, Tenorio-Tagle, & Yorke 1979; Franco, Tenorio-Tagle, & Bodenheimer 1990). High spatial resolution infrared and radio recombination line observations toward several sources have found ionized gas accelerating away from the central source in the manner expected of champagne-flow models (e.g., Garay, Lizano, & Gómez 1994; Keto et al. 1995; Lumsden & Hoare 1996; Lebrón, Rodríguez, & Lizano 2001). Note that in several of the observed compact H II regions (e.g., G 29.96−0.02, G 32.80+0.19B, G 61.48+0.09B1) the inferred rate of ionizing photons implies excitation by central stars with masses $M_* > 30\,M_\odot$.

Density profiles in massive molecular cores have also been extensively studied observationally (e.g., Garay & Rodríguez 1990; Caselli & Myers 1995; Van der Tak et al. 2000; Hatchell et al. 2000; for a review see Garay & Lizano 1999). Even though the environment is possibly clumpy on scales of tenths of pc, density profiles are well approximated by power laws with $1 \lesssim n \lesssim 2$. Theoretical models of the formation of massive stars within dense and massive cores have assumed power law exponents in this range (Osorio, Lizano, & D'Alessio 1999; McKee & Tan 2002). Recently, Franco et al. (2000) have argued that radio continuum spectra of ultracompact H II regions indicate initial density gradients with $2 \lesssim n \lesssim 3$.

The purpose of this paper is to discuss the self-similar "champagne phase" of the expansion of H II regions found by SLGCL, for molecular cloud cores with power-law density distributions with exponents in the range $3/2 < n < 3$. These self-similar models have a shock propagating at constant velocity into the ionized gas, accelerating the gas to supersonic velocities. We will discuss the self-similar equations and solutions in § 2 and § 3 respectively; in § 4 we will consider the evolution of the stellar winds inside these champagne flows; finally, in § 5 we will summarize the results.

2. GOVERNING EQUATIONS

Neglecting the self-gravity of the cloud core and the gravity of the central massive star, the expansion of champagne flows is governed by the continuity equation,

$$\frac{\partial \rho}{\partial t} + \frac{1}{r^2}\frac{\partial\left(r^2 \rho u\right)}{\partial r} = 0, \tag{8}$$

where ρ is the gas density and u is the gas velocity, and by the momentum equation,

$$\frac{\partial u}{\partial t} + u\frac{\partial u}{\partial r} = -\frac{a^2}{\rho}\frac{\partial \rho}{\partial r}, \tag{9}$$

where an isothermal equation of state $P = a^2\rho$ was assumed.

Following Shu (1977) we introduce the similarity variable

$$x = \frac{r}{at}, \tag{10}$$

and we define the reduced density

$$\rho(r,t) = \frac{K}{r^n}R(x), \tag{11}$$

and the reduced velocity

$$u(r,t) = av(x). \tag{12}$$

Substituting these expressions in equations (8) and (9), one obtains two coupled first order differential equations for the reduced density R and velocity v:

$$\left[(v-x)^2 - 1\right]\frac{dR}{dx} = \frac{R}{x}\left[v(v-x)(n-2) - n\right], \tag{13}$$

$$\left[(v-x)^2 - 1\right]\frac{dv}{dx} = \frac{2v}{x} - n. \tag{14}$$

The heating of the cloud at $t = 0$ induces an imbalance between the self-gravity and pressure that will induce the propagation of a shock and an outward subsonic flow of the entire system for $t > 0$. SLGCL showed that the shock is isothermal, thus the jump conditions are

$$(v_{\rm u} - x_{\rm s})(v_{\rm d} - x_{\rm s}) = 1, \quad \frac{R_{\rm d}}{R_{\rm u}} = (v_{\rm u} - x_{\rm s})^2, \tag{15}$$

where the subscript 'u' ('d') indicates the value of the reduced velocity and density upstream (downstream) of the shock and $x_{\rm s}$ is the position of the shock in similarity coordinates. From equation (10) the position and velocity of the shock in physical space are $r_{\rm s} = x_{\rm s}at$ and $u_{\rm s} \equiv dr_{\rm s}/dt = ax_{\rm s}$.

For $x \to \infty$ the boundary conditions are $v \to 0$ and $R \to 1$. Then, the asymptotic expansions for $x \to \infty$, are

$$v \to \frac{n}{x} \quad \text{and} \quad R \to 1 + \frac{n(n-1)}{2x^2}. \tag{16}$$

At the origin, $x \to 0$, $v \to nx/3$ and $R \propto x^n$. The latter boundary condition on R implies that as $r \to 0$ the density is uniform and is only a function of time $\rho \propto t^{-n}$. This is the expected behavior of the central zone of the H II region, where the sound crossing time is smaller than the expansion time.

Equation (14) for the reduced velocity can be integrated numerically outward from $x = 0$ and inward from large x. The position of the shock, $x_{\rm s}$, is found where the jump conditions (equation 15) are fulfilled. Once the reduced velocity v is known, the density equation (13) can be integrated as

$$R(x) = R_{\rm b}\exp\left\{\int_{x_{\rm b}}^{x} \frac{v\,(v-x')\,(n-2) - n}{x'\left[(v-x')^2 - 1\right]}\,dx'\right\}. \tag{17}$$

For the outer solution, $x_{\rm b} = \infty$ and $R_{\rm b} = 1$. For the inner solution, $x_{\rm b} = x_{\rm s}$ and $R_{\rm b} = R_{\rm d}$, where $R_{\rm d}$ is the downstream reduced density evaluated from the jump condition (equation 15).

3. OUTFLOW SOLUTIONS FOR DIFFERENT GRADIENTS

The upper panel of Figure 1 shows the reduced velocity v for $n = 2$. The position of the shock front is at $x_{\rm s} = 2.56$ and the upstream reduced velocity, due to the cloud general expansion, is $v_{\rm u} = 1.02$. The dotted line shows the locus of the critical line where the LHS of equation (14) vanishes. The lower panel of Fig. 1 shows the reduced density R. The dashed line shows the function $R = 3(x/x_{\rm s})^2$, which corresponds to a region of uniform but steadily decreasing density, given by spreading the original gaseous mass interior to $r_{\rm s} = x_{\rm s}at$ evenly over the enclosed spherical volume. Except for a slight increase of R from its average interior value of 3 to the post-shock value $R_{\rm d} = 3.20$ just downstream from the shock front at $x = x_{\rm s}$, Fig. 1 shows that the high gaseous pressure does a fairly good job of ironing out pressure differences in the interior volume.

Figure 2 show the analogous reduced velocity v and density R for $n = 2.99$. The dotted line in the upper panel corresponds to the critical line. In this

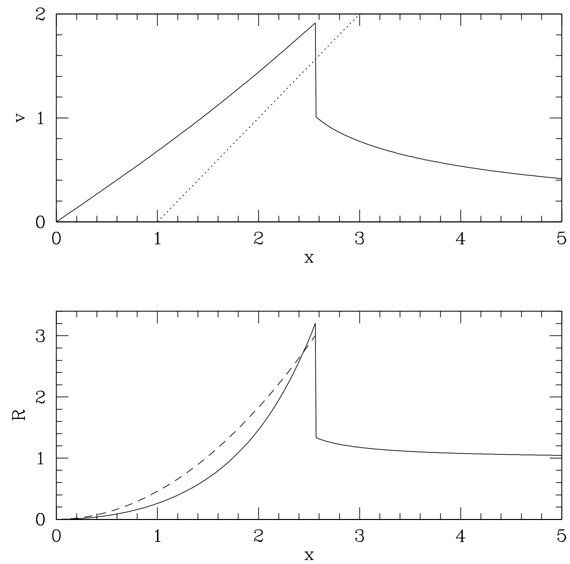

Fig. 1. *Top panel:* reduced velocity v for the exponent $n = 2$. The dotted line is the critical line $v = x - 1$. The shock front is at $x_s = 2.56$. The pre-shock velocity is $v_1 = 1.02$. *Bottom panel:* reduced density R. The dashed curve corresponds to $R = 3(x/x_s)^2$ and shows the deviation from uniform density.

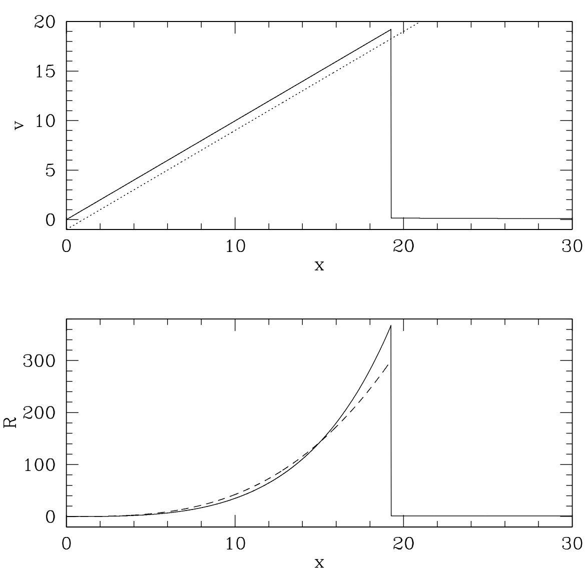

Fig. 2. *Top panel:* reduced velocity v for the exponent $n = 2.99$. The dotted line is the critical line $v = x - 1$. The shock front is at $x_s = 19.25$. The pre-shock velocity is only $v_1 = 0.16$. *Bottom panel:* reduced density R. The dashed line corresponds to $R = 300(x/x_s)^{2.99}$ and shows the deviation from uniform density.

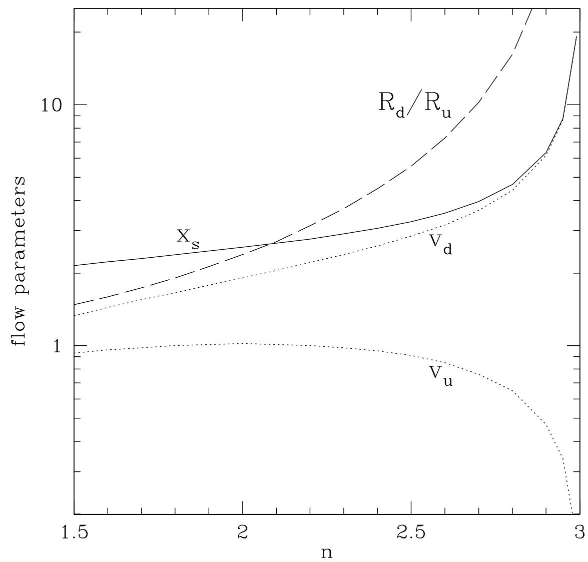

Fig. 3. Results of the models as a function of n. The solid line shows the position of the shock x_s, the upper and lower broken lines show the post-shock and pre-shock reduced velocities (v_d, v_u) respectively, and the long-dashed line shows the ratio of the post-shock and pre-shock reduced densities, R_d/R_u.

case the shock front is at $x_s = 19.25$. This number is also the velocity of the shock wave relative to the isothermal sound speed of the H II region. In contrast, the pre-shock velocity of the gas (relative to the origin) is only $v_u = 0.16$, because at a given spatial position there is less time for the cloud to expand before the shock arrives. The reduced density R in the lower panel has a correspondingly large post-shock density increase. The dashed line shows the function

$$R = \left(\frac{3}{3-n}\right)\left(\frac{x}{x_s}\right)^n, \tag{18}$$

with $n = 2.99$, given by spreading the original gaseous mass interior to $r_s = x_s at$ evenly over the enclosed spherical volume. Fig. 2 shows that the shock dynamics raises the immediate downstream value from the average expectation $3/(3-n) = 300$ at $x = x_s$ to the actual postshock value $R_d = 368$.

Figure 3 summarizes the results for the self-similar models with different power-law density exponents n. The solid line shows the position of the shock x_s; the upper and lower dotted lines show the post-shock and pre-shock reduced velocities (v_d, v_u) respectively; and the long-dashed line shows the ratio of the post-shock and pre-shock reduced densities R_d/R_u. One can see that x_s increases as $n \to 3$.

For the case $n = 3$, equations (13) and (14) have the analytic solution $R = Cx^3$ and $v = x$, where C is an arbitrary constant. The jump conditions (equation 15) imply that $x_{\rm s} \to \infty$ as $v_{\rm d} \to x$. Thus, in spatial coordinates the shock front, $r_{\rm s} = x_{\rm s}at$, and the shock velocity, $u_{\rm s} = ax_{\rm s}$, go to infinity. SLGCL showed that the shock velocity diverges as $n \to 3$ because the model includes the origin, where the pressure driving the shock diverges. If one integrates instead from the radius of influence r_0, for $n < 3$ the shock speed tends to the constant speed of the self-similar models. On the other hand, for the case $n \geq 3$, the shock accelerates to ∞ as $r_{\rm s} \to \infty$. As the velocity increases, the assumptions of the model will, of course, eventually break down.

4. STELLAR WINDS INSIDE CHAMPAGNE FLOWS

Massive stars are expected to turn on powerful winds very early in their lives. As shown above, the density of the champagne flow tends to become uniform in the center (equation 18). Thus, following Garay et al. (1994) who studied the evolution of stellar winds inside champagne flows, we assume that the stellar wind evolves into a medium of uniform density given

$$\overline{\rho}(t) = \frac{\int_0^{r_{\rm s}} 4\pi r^2 \rho(r,t)\, dr}{\int_0^{r_{\rm s}} 4\pi r^2\, dr} = \left(\frac{3}{3-n}\right) \rho[r_{\rm s}(t)], \quad (19)$$

where $r_{\rm s}(t) = x_{\rm s}at$ is the instantaneous position of the shock front and $n < 3$. In this case, the equations of mass conservation, momentum, and energy of the snow-plow phase (Castor, McCray, & Weaver 1975) allow power-law solutions for the radius of the swept-up shell, $r_{\rm w}$, driven by a hot bubble of shocked stellar wind. In our notation

$$r_{\rm w} = \left[\frac{125(3-n)(9-2n)}{3(3+n)^2(7-n)(11+2n)}\right]^{1/5} \times \left[\frac{L_{\rm w}(x_{\rm s}a)^n}{2\pi K}\right]^{1/5} t^{(3+n)/5}, \quad (20)$$

where $L_{\rm w} = \frac{1}{2}\dot{M}_{\rm w}u_{\rm w}^2$ is the wind luminosity, $\dot{M}_{\rm w}$ is the wind mass-loss rate, and $u_{\rm w}$ is the stellar wind speed, assumed constant. Comparing this expression for the wind radius with the value of the shock radius $r_{\rm s} = x_{\rm s}at$, we see that for $n \leq 2$ the stellar wind can remain confined inside the champagne flow (champagne-dominated flow), whereas for $n > 2$ it accelerates and eventually overtakes the champagne flow (wind-dominated flow).

In the particular case $n = 2$ both $r_{\rm s}$ and $r_{\rm w}$ increase linearly with time. In terms of the self-similar variable equation (10), one can then write

$$r_{\rm w}(t) = x_{\rm w}\, a\, t, \quad (21)$$

where $x_{\rm w}$ is given by equation (20) for $n = 2$,

$$x_{\rm w} = \left[\frac{L_{\rm w}\, x_{\rm s}^2}{18\pi\, a^3\, K}\right]^{1/5}. \quad (22)$$

For a stellar wind with $L_{\rm w} \simeq 10^{36}\,{\rm erg\,s^{-1}}$, and for typical density parameters of massive cores, $K \simeq 10^{16}\,{\rm g\,cm^{-1}}$, and $a \simeq 10\,{\rm km\,s^{-1}}$, one obtains $x_{\rm w} = 1.62$. Since $x_{\rm s} = 2.56$, the stellar wind (moving at $u_{\rm w} \simeq 16\,{\rm km\,s^{-1}}$) remains inside the champagne flow induced by the passage of the shock (moving at $u_{\rm s} \simeq 26\,{\rm km\,s^{-1}}$).

One can refine this estimate by relaxing the assumption of uniform density (equation 19), and using instead the actual density profile $R(x)$ established in the cloud by the passage of the shock. In this case the snow-plow phase equations give, for $n = 2$, a transcendental equation for $x_{\rm w}$

$$x_{\rm w} = \left[\frac{L_{\rm w}}{6\pi\, a^3\, K\, R(x_{\rm w})}\right]^{1/3}. \quad (23)$$

For the values of the physical parameters given above one obtains $x_{\rm w} = 1.74$, in good agreement with the previous estimate. The condition to have a champagne-dominated flow as opposed to a stellar-wind-dominated flow is given by the requirement $x_{\rm w} = x_{\rm s}$, i.e.,

$$\frac{L_{\rm w}}{6\pi\, K\, a^3} < R(x_{\rm s})\, x_{\rm s}^3 \simeq 54, \quad (24)$$

where $x_{\rm s} = 2.56$ and $R(x_{\rm s}) = 3.20$ (see Fig. 3). For the range of parameters $(L_{\rm w}, K)$ that can keep the stellar wind confined inside the champagne flow, the exact solution, equation (23), for $n = 2$ and the solution, equation (22), obtained using the mean density differ by less than 10% . We are therefore confident that equation (20) can be used to estimate the evolution of winds inside champagne flows of different power-law exponents n. In particular, a wind dominated H II region like Orion possibly had an original density distribution with a density slope steeper than $n = 2$, as expected at the edges of molecular clouds.

5. SUMMARY

We have discussed the self-similar models of champagne flows found by SLGCL. These models show that when a molecular core is ionized and heated out of equilibrium, steep density gradients characteristic of star-forming regions produce shocks that travel at constant velocity and accelerate the ionized gas to supersonic speeds. We showed here that is it possible to take into account the evolution of the stellar wind driven bubble of hot shocked gas inside the champagne flow. For cloud core density power-law exponent $n \leq 2$, the swept-up wind shell can be confined inside the champagne flow. For $n > 2$, the wind shell accelerates and eventually overtakes the champagne shock.

One problem found by SLGCL is that, due to the supersonic expansion of champagne flows, the emission measure decreases rapidly and in a short time the source fades away from observational classification as a compact H II region. These latter sources have values of the emission measure (EM) in the range $10^6\,\mathrm{cm}^{-6}\,\mathrm{pc} \lesssim \mathrm{EM} \lesssim 10^8\,\mathrm{cm}^{-6}\,\mathrm{pc}$ (e.g., Garay et al. 1994). The stellar winds discussed here would only exacerbate the situation. They proposed that a continuous source of ionized mass is required to keep up the density of the expanding champagne flow. Photoevaporation of circumstellar disks (Hollenbach et al. 1994; Richling & Yorke 1997) or mass loading by the photoevaporation and/or hydrodynamic ablation of remnant neutral globules surrounding the central star (e.g., Lizano et al. 1996; Redman, Williams, & Dyson 1996) are natural solutions to maintain the high observed emission measures in champagne flows and, in general, in ultracompact H II regions.

We thank Frank Wilkin and Bob O'Dell for very useful discussions. S. L. and J. C. acknowledge support from DGAPA/UNAM and CONACyT. F. S. acknowledges support in the United States from the NSF and NASA, and in Taiwan from the National Science Council. D. G. acknowledges support from grant COFIN-2000.

REFERENCES

Bodenheimer, P., Tenorio-Tagle, G., & Yorke, P. 1979, ApJ, 233, 85
Caselli, P., & Myers, P. 1995, ApJ, 446, 665
Castor, J., McCray, R., & Weaver, R. 1975, ApJ, 200, L107
Franco, J., Kurtz, S., Hofner, P., & Testi, L. 2000, ApJ, L143
Franco, J., Tenorio-Tagle, G., & Bodenheimer, P. 1990, ApJ, 349, 126
Garay, G., & Lizano, S. 1999, PASP, 111, 1049
Garay, G., Lizano, S., & Gómez, Y. 1994, ApJ, 429, 268
Garay, G., & Rodríguez, L. F. 1990, ApJ, 362, 191
Hatchell, J., Fuller, G. A., Millar, T. J., Thompson. M. A., & Macdonald, G. H. 2000, A&A, 357, 637
Hollenbach, D., Johnstone, D., Lizano, S., & Shu, F. H. 1994, ApJ, 428, 654
Keto, E. R., Welch, W. J., Reid, M. J., & Ho, P. T. P. 1995, ApJ, 444, 765
Lebrón, M., Rodríguez, L. F., & Lizano, S. 2001, ApJ, 560, 806
Lizano, S., Cantó, J., Garay, G., & Hollenbach, D. 1996, ApJ, 739
Lumsden, S. L., & Hoare, M. G. 1996, ApJ, 464, 272
McKee, C., & Tan, J. C. 2002, Nature, 416, 59
Osorio, M., Lizano, S., & D'Alessio, P. 1999, ApJ, 525 808
Osterbrok, D. E. 1989, Astrophysics of Gaseous Nebulae and Active Galactic Nuclei (Mill Valley: University Science Books)
Redman, M. P., Williams, R. J. R., & Dyson, J. E. 1996, MNRAS, 280, 661
Richling, S., & Yorke, H. W. 1997, A&A, 327, 317
Shu, F. 1977, ApJ, 214, 488
Shu, F., Lizano, S., Galli, D., Cantó, J., & Laughlin, G. 2002, ApJ, 580, 969 (SLGCL)
Strömgren, B. 1939, ApJ, 89, 526
Vacca, W. D., Garmany, C. D., & Shull, J. M. 1996, ApJ, 460, 914
van der Tak, F. F. S., van Dishoeck, E. F., Evans, N. J. II, & Blake, G. A. 2000, ApJ 537, 283

Jorge Cantó: Instituto de Astronomía, Universidad Nacional Autónoma de México, Apartado Postal 70-264, 04510 México, D. F., México.
Daniele Galli: Osservatorio Astrofisico di Arcetri, Largo Enrico Fermi 5, I-50125 Firenze, Italy (galli@arcetri.astro.it).
Susana Lizano: Instituto de Astronomía, Universidad Nacional Autónoma de México, Campus Morelia, Apartado Postal 3-72, 58090 Morelia, Michoacán, México (s.lizano@astrosmo.unam.mx).
Frank Shu: National Tsing Hua University, 101 Section 2 Kuang Fu Road, Hsinchu, Taiwan 30013, ROC (shu@astron.berkeley.edu).